

Potent Antitrypanosomal Activities of Heat Shock Protein 90 Inhibitors In Vitro and In Vivo

Kirsten J. Meyer¹ and Theresa A. Shapiro^{1,2}

¹Department of Pharmacology and Molecular Sciences and ²Division of Clinical Pharmacology, Department of Medicine, The Johns Hopkins University School of Medicine, Baltimore, Maryland

African sleeping sickness, caused by the protozoan parasite *Trypanosoma brucei*, is universally fatal if untreated, and current drugs are limited by severe toxicities and difficult administration. New antitrypanosomals are greatly needed. Heat shock protein 90 (Hsp90) is a conserved and ubiquitously expressed molecular chaperone essential for stress responses and cellular signaling. We investigated Hsp90 inhibitors for their antitrypanosomal activity. Geldanamycin and radicicol had nanomolar potency in vitro against bloodstream-form *T. brucei*; novobiocin had micromolar activity. In structure-activity studies of geldanamycin analogs, 17-AAG and 17-DMAG were most selective against *T. brucei* as compared to mammalian cells. 17-AAG treatment sensitized trypanosomes to heat shock and caused severe morphological abnormalities and cell cycle disruption. Both oral and parenteral 17-DMAG cured mice of a normally lethal infection of *T. brucei*. These promising results support the use of inhibitors to study Hsp90 function in trypanosomes and to expand current clinical development of Hsp90 inhibitors to include *T. brucei*.

Keywords. *Trypanosoma brucei*; human African trypanosomiasis; Hsp90; inhibitor; drug; kinetoplast; cell cycle; geldanamycin; 17-AAG; 17-DMAG.

African sleeping sickness (human African trypanosomiasis; HAT) is caused by the protozoan kinetoplastid parasite *Trypanosoma brucei* [1]. Kinetoplastids, including the human pathogens *Trypanosoma cruzi* and *Leishmania* species, are early diverging eukaryotes named for the kinetoplast, the characteristic dense granule of DNA at the base of the flagellum that comprises the mitochondrial genome. *T. brucei* is transmitted by the tsetse fly and causes endemic disease in both livestock (nagana) and humans (HAT) in sub-Saharan Africa. The parasite propagates extracellularly and moves throughout the body, including the central nervous system during the late stage of disease. In

humans, this infection is fatal unless treated. Current therapies require repeated parenteral dosing and have formidable toxicities, exemplified by the 5%–10% lethality caused by the commonly used drug melarsoprol. New antitrypanosomal drugs are long overdue.

Heat shock protein 90 (Hsp90) is a phylogenetically conserved, abundant, and essential molecular chaperone [2–7]. In mammalian cells it functions as a homodimer complexed with regulatory cochaperones. Hsp90 stabilizes substrate (ie, client) proteins, enabling their proper activities. Over 200 clients have been identified, with many acting in signal transduction pathways, stress responses, and cell cycle regulation [4]. Thus, Hsp90 is a critical node coordinating many networks necessary for survival. This combinatorial function and a disproportionate dependence on Hsp90 activity in malignant cells have established it as a cancer chemotherapy target [5–8]. Dozens of Hsp90 inhibitors have entered the drug development pathway, including derivatives of the natural products geldanamycin (eg, 17-AAG [17-*N*-allylamino-17-demethoxygeldanamycin] and 17-DMAG [17-dimethylaminoethylamino-17-demethoxygeldanamycin]) and radicicol, as well as novel structural scaffolds identified in screens. 17-AAG has

Received 26 December 2012; accepted 5 February 2013; electronically published 22 April 2013.

Presented in part: 23rd Molecular Parasitology Meeting, Abstract 5B, Woods Hole, Massachusetts, 22–26 September 2012.

Correspondence: Theresa Shapiro, MD, PhD, Division of Clinical Pharmacology, Department of Medicine, The Johns Hopkins University School of Medicine, 301 Hunterian Bldg, 725 N Wolfe St, Baltimore, MD 21205-2185 (tshapiro@jhmi.edu).

The Journal of Infectious Diseases 2013;208:489–99

© The Author 2013. Published by Oxford University Press on behalf of the Infectious Diseases Society of America. All rights reserved. For Permissions, please e-mail: journals.permissions@oup.com.

DOI: 10.1093/infdis/jit179

been in phase 3 trials [6]. Geldanamycin treatment leads to proteosomal degradation of Hsp90 client proteins, cell cycle arrest, and heat shock response in mammalian cells [9]. Damage to multiple proteins and pathways may be the basis for reported synergism between Hsp90 inhibitors and several chemotherapeutic agents [10].

The kinetoplastid homologue of Hsp90 is Hsp83, and there are 10 tandem copies in the *T. brucei* genome [11]. Hsp83 influences the temperature-sensitive differentiation of insect to mammalian-form *Leishmania* organisms and *T. cruzi* [12, 13], and Hsp90 inhibitors arrest the growth of several kinetoplastids in vitro and have activity against *Trypanosoma evansi* in mice [12–16]. However, little is known about the role of Hsp83 in cellular metabolism and its clients and cochaperones remain to be identified. Initial studies have found that Hsp83 interacts with the deacetylase Sir2 in *Leishmania* organisms and with protein phosphatase 5 in *T. brucei* [15, 17]. Although the trypanosome genome lacks evidence of steroid hormone receptors and tyrosine kinases that are prominent Hsp90 clients in mammalian cells, homologues of other clients are recognizable, including serine/threonine kinases and cell cycle regulators [18, 19].

The cell cycle of kinetoplastids differs dramatically from that of host cells. In trypanosomes, the replication of mitochondrial DNA (the kinetoplast) occurs once, and its S, G₂, and M phases precede those of nuclear DNA (Figure 1A) [20–22]. The Golgi, basal bodies, and flagellum are also replicated in an ordered fashion and then precisely positioned so cytokinesis can occur via cleavage furrow ingression. The complex temporal requirements of these processes, coupled with a lack of tight checkpoints characteristic in higher eukaryotes [23], make trypanosomes particularly vulnerable to cell cycle disaster [24].

We evaluated structurally diverse Hsp90 inhibitors, including some already studied in humans, for their activity against bloodstream-form trypanosomes in vitro, explored structure-activity relationships for the geldanamycin scaffold, assessed the effect of inhibitors on the cell cycle, tested 17-AAG in combination with other drugs, and demonstrated the efficacy of orally dosed 17-DMAG against *T. brucei* infection in mice.

MATERIALS AND METHODS

Cell Culture, Reagents, and Cytotoxicity Assay

All studies used bloodstream *T. brucei brucei* (MiTat 1.2 strain 427) maintained continuously in exponential growth (10^4 – 10^5 cells/mL) at 37°C and 5% CO₂ in phenol red-free HMI-9, 10% fetal bovine serum (Invitrogen), and 10% Serum Plus (SAFC Biosciences). Motile parasites were counted by a hemocytometer. L1210 murine leukemia cells (ATCC CCL-219) were maintained in phenol red-free Roswell Park Memorial Institute 1640 medium (Sigma-Aldrich) and 15% fetal bovine serum. Stock solutions of compounds were aliquoted and stored at

–20°C, as follows: radicicol (Sigma-Aldrich) and ansamycins (including geldanamycin, 17-AAG, and 17-DMAG; The NCI/DTP Open Chemical Repository [available at: <http://dtp.cancer.gov>]) in sterile dimethyl sulfoxide (DMSO; Hybri-Max, Sigma-Aldrich); novobiocin (Sigma-Aldrich), eflornithine (NCI/DTP), and pentamidine (Lymphomed) in H₂O; and melarprol (Centers for Disease Control and Prevention) in 1,2-propanediol (Sigma-Aldrich). Final DMSO percentage of $\leq 0.5\%$ had no effect in the cytotoxicity assay. Cytotoxicity was assayed by a colorimetric 96-well plate acid-phosphatase method [25]. Cells were exposed to compound for 24 hours (*T. brucei* seeding concentration, 1×10^5 cells/mL) or 48 hours (L1210 seeding concentration, 7×10^4 cells/mL), reflecting respective doubling-times of 6 and 11 hours. Dose-response curves and half-maximal effective concentrations (EC₅₀ values) were obtained (Microsoft Excel and DeltaGraph Pro v3.5).

Flow Cytometry

For each time point, 3×10^6 cells from treated cultures (seeded at 2×10^5 cells/mL) were pelleted at $1000 \times g$ for 10 minutes; washed twice with glucose- and sucrose-supplemented phosphate-buffered saline (vPBS) [26]; fixed by dropwise addition of ice-cold 70% EtOH in PBS; and stored at 4°C. Cells were pelleted at $3000 \times g$ for 10 minutes, washed with PBS, resuspended in 500 μ L 10 μ g/mL RNaseA in PBS, and incubated at 37°C for 45 minutes. After addition of propidium iodide (Sigma-Aldrich) to achieve a final concentration of 20 μ g/mL, 10 000 cells were analyzed on FACSCalibur (BD Biosciences), gated on FL2-A versus FL2-W to exclude doublets, and the G₁ peak of controls was centered at 200 units FL2-A (CellQuest Pro v5.2, BD Biosciences).

DAPI Staining and Microscopy

For each time point, 2×10^6 cells from treated cultures seeded at 2×10^5 cells/mL were pelleted at $1000 \times g$ for 10 minutes, washed with vPBS, fixed with 3% paraformaldehyde in PBS for 10 minutes on ice, diluted 5-fold in vPBS, pelleted at $3000 \times g$ for 10 minutes, washed with vPBS, applied to polylysine-coated slides for 1 hour, permeabilized with 0.1% Triton X-100 (Sigma-Aldrich) in PBS for 10 minutes, washed thrice with PBS, and mounted using Fluoroshield with DAPI (Sigma-Aldrich) [26]. Slides were imaged on a Zeiss Axioskop with a Retiga Exi charge-coupled-device camera (QImaging), using iVision v4.0.13 (Biovision Technologies). Images were merged and adjusted for brightness and contrast only (ImageJ v1.45s, Rasband). For quantitation, images of ≥ 100 cells/condition were randomized then scored by 3 blinded independent observers with respect to the number of nuclei and kinetoplasts and the appearance by fluorescence and/or phase.

Animal Studies

Protocols were approved by the Johns Hopkins Institutional Animal Care and Use Committee. Drug solutions were

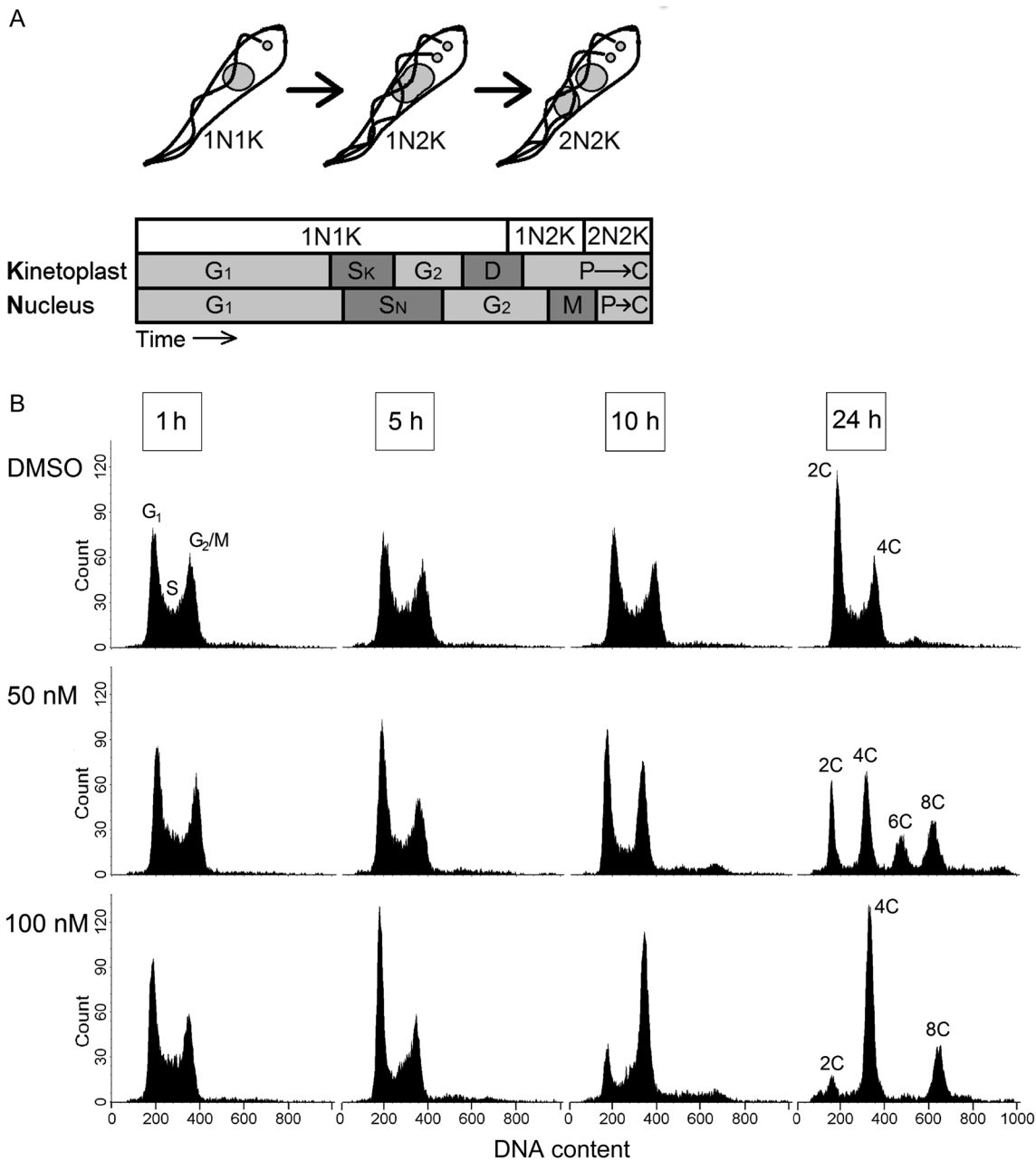
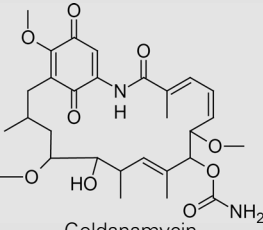
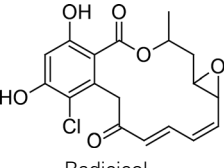
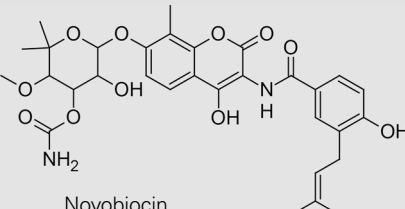


Figure 1. The cell cycle of *Trypanosoma brucei* is disrupted by 17-AAG. **A**, In trypanosomes both the nuclear and the mitochondrial genomes can be visualized by light microscopy, and their replication is temporally linked but not strictly synchronous. Cells progress from having 1 nucleus and kinetoplast (1N1K), to having 1 nucleus and 2 kinetoplasts (1N2K), and finally to having 2 nuclei and kinetoplasts (2N2K) before the cells divide by cleavage furrow ingression to yield 2 daughter cells (adapted from [20, 22]). G₁, gap 1; S_{K/N}, synthesis kinetoplast/nuclear DNA; G₂, gap 2; D, kinetoplast division; M, nuclear mitosis; P, positioning of organelles, C, cytokinesis. **B**, Trypanosomes were treated with solvent, 50 nM 17-AAG, or 100 nM 17-AAG for the indicated times and then examined by flow cytometry. Since the kinetoplast composes only 5% of the total cellular DNA [32], this method focuses on the nuclear genome. DMSO, dimethyl sulfoxide; 2C, nonreplicating diploid cells with 2 copies of nuclear genomic DNA; 4C, cells late in replication with 4 copies of genomic DNA; 6C or 8C, abnormal cells with 6 or 8 copies of the nuclear genome.

prepared immediately before use in 5% glucose vehicle. Six-week-old female CD1 mice were infected with *T. brucei* (MiTat 1.2 strain 427; 5×10^4) intraperitoneally on day 0. On day 1, after confirmation of parasitemia, animals were divided into

groups of 3 (groups 1–4) or 4 (group 5) and then treated once daily with vehicle (200 μ L intraperitoneally for 3 days; group 1), 3.5 mg/kg Berenil (Sigma–Aldrich; 200 μ L intraperitoneally for 3 days; group 2), 150 mg/kg 17-DMAG (400 μ L

Table 1. Activity of Heat Shock Protein 90 Inhibitors Against Trypanosomes In Vitro

Compound	EC ₅₀ (nM) ^a
 Geldanamycin	12 ± 4
 Radicol	70 ± 14
 Novobiocin	180 000 ± 21 000

Abbreviation: EC₅₀, half maximal effective concentration

^a Values are mean ± SD of at least 3 independent experiments. *r*² values for dose-response curves all exceeded 0.99; within an assay, the coefficients of variation for quadruplicate determinations were all ≤10% and averaged 1.8%.

intraperitoneally once; group 3), 30 mg/kg 17-DMAG (200 μL intraperitoneally for 5 days; group 4), or 50 mg/kg 17-DMAG (200 μL by oral gavage for 5 days; group 5). Mice were weighed prior to infection and daily during the first week; parasitemia was monitored in tail snip blood samples for 30 days. Mice with >5 × 10⁸ trypanosomes/mL or in evident distress were euthanized.

RESULTS

In Vitro Antitrypanosomal Activity of Parent Compounds

Initial studies were designed to determine whether structurally diverse Hsp90 inhibitors had cytotoxic activity against African trypanosomes in vitro. Geldanamycin and radicol both bind to the *N*-terminal adenosine triphosphate (ATP)-binding pocket, which has a rare Bergerat-fold, of Hsp90 and inhibit ATPase activity [27, 28]. Novobiocin binds the *C*-terminal domain [29]. Geldanamycin and radicol had potent nanomolar EC₅₀ values against *T. brucei* (Table 1), in agreement with reported 50% growth inhibition at 40 nM geldanamycin [15]. Novobiocin had micromolar activity. For comparison, clinically used antitrypanosomals pentamidine, melarsoprol, and

eflornithine had EC₅₀ values of 7 nM, 10 nM, and 50 μM, respectively, in this assay. Geldanamycin and radicol values fall well within this range.

Structure Activity Relationships on the Ansamycin Scaffold

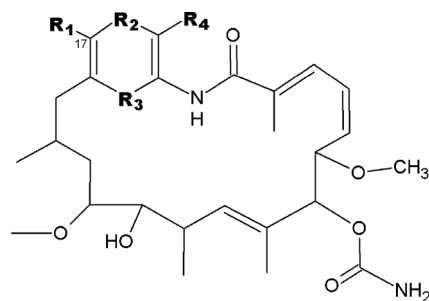
On the basis of the impressive potency of geldanamycin, 12 related ansamycins were analyzed for structure-activity relationships (Tables 2 and 3). For some measure of therapeutic index, compounds were also evaluated against L1210 mammalian cells. Disruption of the geldanamycin quinone (compound 255108; Table 2) reduced activity severely against trypanosomes and moderately against L1210. Sterically demanding hydrazone moieties at R₄ (210753, 255112, and 265482) substantially decreased activity against both cell types. Modifications at C17 were well tolerated. Replacement of the methoxy at R₁ with a hydroxyl group (255104) decreased potency by 10-fold against both cell types, but incorporation of a chloroethylamino group (320877) had little to no effect on potency. Importantly, however, other amino moieties at R₁ enhanced selective toxicity against trypanosomes: a primary amine (255109) or allyl amino group (330507) resulted in a 30–50-fold increase in selectivity, and a dimethylaminoethylamino group (707545) increased selectivity 300-fold. An even more substantial change, a large, rigid bromo-benzoxazine bridging positions R₁ and R₂ (255105), maintained good activity against both cell types, suggesting that this position is not constrained in the drug and target interaction. Modifications in more remote ansamycin ring substituents and reduction of the quinone (330500; Table 3) impaired potency and selectivity, while opening the macrocycle (265481) resulted in complete loss of activity.

The general trends of these structure activity relationships correlate with crystal structure data of ansamycins complexed with Hsp90, where C17 modifications are exposed to solvent and outside the Bergerat-fold ATP-binding pocket [30]. However, the series also reveals differences in the susceptibility of mammalian and trypanosome cells. Many factors may account for this, including phylogenetic differences in the target enzymes. This possibility is supported by the several-log difference in ATPase activity of kinetoplastid Hsp83, compared with mammalian Hsp90 [31]. Compounds with the most favorable selectivity were 17-AG (255109), 17-AAG (330507), and 17-DMAG (707545); the latter was also most potent against trypanosomes. As 17-AAG is the most widely studied, we chose to characterize its antitrypanosomal effect more fully.

17-AAG Affects Growth Rate, Mitosis, and Cytokinesis

Previous reports indicate that, for insect-form *T. cruzi* or *Leishmania donovani*, 24 hours geldanamycin treatment arrests the cell cycle at either G₁ or G₂ [12–14]. We found that, within 5 hours, 50 or 100 nM 17-AAG (EC₈₀ or EC₉₉, respectively) arrested growth of bloodstream *T. brucei*, and cell numbers declined thereafter (Supplementary Figure 1A). Cell cycle

Table 2. Structure Activity Relationships of Ansamycins



Ansamycin Scaffold

NSC Number	Modification				EC ₅₀ (nM) ^a		
	R1	R2	R3	R4	<i>T. brucei</i>	L1210	Selectivity ^b
122750 Geldanamycin	OCH ₃	CO	CO	H	13	12	1
255108	OCH ₃			H	38 000	7100	0.2 ^c
210753	OCH ₃	CO	CO		2800	940	0.3 ^c
255112	OCH ₃	CO	CO		13 000	9600	0.7
265482	OCH ₃	CO	CO		3400	5800	2
255104	OH	CO	CO	H	130	180	1
320877		CO	CO	H	17	21	1
255109	NH ₂	CO	CO	H	6.0	180	30 ^c
330507 17-AAG		CO	CO	H	38	1800	50 ^c
707545 17-DMAG		CO	CO	H	3.1	1000	300 ^c
255105			CO	H	27	23	0.9

Abbreviations: EC₅₀, half maximal effective concentration; *T. brucei*, *Trypanosoma brucei*.

^a Values are mean of at least 3 independent determinations. Coefficients of variation for EC₅₀ values were all ≤33%. *r*² values for dose-response curves all exceeded 0.98; within an assay, the coefficients of variation for quadruplicate determinations were ≤10% and averaged 2.1%.

^b Defined as the ratio of the L1210 EC₅₀ to the *T. brucei* EC₅₀; large numbers are favorable.

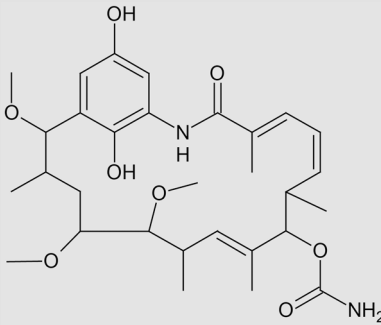
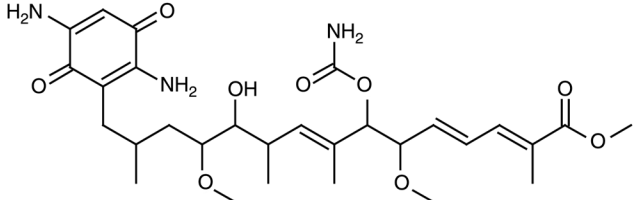
^c *P* < .05, by a 2-tailed *t* test, for comparison of *T. brucei* and L1210 values.

progression was inhibited, and this was examined by flow cytometry and microscopy of DAPI-stained cells, across time and concentration.

On the basis of nuclear DNA content, as measured by flow cytometry, control cultures in mid-log growth were 38% G₁ (2C DNA content for the diploid trypanosome), 21% S, and 35% G₂/M (4C DNA content). This distribution was maintained until the culture reached stationary phase at 24 hours (Figure 1B). Treatment with 50 nM 17-AAG caused a transient increase in the G₁ peak at 5 hours, which decreased

progressively thereafter. At 10 hours the G₂/M (or 4C) peak was increased, indicating a problem with mitosis and/or cytokinesis. At 24 hours, the 4C peak remained significant, but substantial 6C and 8C peaks were also present. These abnormal forms are possible in bloodstream trypanosomes because of inadequate or missing checkpoints to stop rereplication of DNA when cytokinesis is delayed or inhibited [23]. With 100 nM 17-AAG, the 5-hour increase in G₁ and 10-hour increase in G₂/M (or 4C) were also seen, but at 24 hours the dominant population was 4C, along with an 8C but no 6C peak. With both

Table 3. Structure Activity Relationships on the Ansamycin Scaffold

NSC Number	Structure	EC ₅₀ (nM) ^a		
		<i>T. brucei</i>	L1210	Selectivity ^b
330500 Macbecin II		240	47	0.2 ^c
265481		>80 000	>80 000	NA

Abbreviations: EC₅₀, half maximal effective concentration; NA, not applicable; *T. brucei*, *Trypanosoma brucei*.

^a Values are mean of at least 3 independent determinations. Coefficients of variation for EC₅₀ values were all ≤35%. *r*² values for dose-response curves all exceeded 0.98; within an assay, the coefficients of variation for quadruplicate determinations were ≤10% and averaged 2.6%.

^b Defined as the ratio of the L1210 EC₅₀ to the *T. brucei* EC₅₀; large numbers are favorable.

^c *P* < .05, by a 2-tailed *t* test.

concentrations, the percentage of cells in S phase declined (quantitations appear in [Supplementary Figure 1B–D](#)).

To obtain further insight into this cell cycle disruption, we examined trypanosomes by fluorescence microscopy. Unlike flow cytometry, which reflects nuclear DNA content, visual analysis of DAPI-stained cells assays both nuclear and kinetoplast DNA, and phase contrast provides concomitant analysis of cytokinesis. Control cells can be divided into 3 populations: 1N1K cells, which have a single nucleus and kinetoplast (68% of the total); 1N2K cells, in which mitochondrial DNA has divided but nuclear mitosis has not occurred (21%); and 2N2K cells, in which the kinetoplast and nucleus have both divided (8%) (Figure [2Ai–iii](#) and [2B](#)). These proportions are in good agreement with flow cytometry: G₁ plus S (38% + 21%) are a subset of 1N1K (68%), and 1N2K plus 2N2K (21% + 8%) are a subset of G₂/M (35%) (Figure [1A](#)). Likewise consistent with flow cytometry, treatment with 50 nM 17-AAG reduced 1N cells and increased 2N cells and forms containing greater than 2N (Figure [2B](#)). Simultaneous accounting for both nuclei and kinetoplasts revealed the vivid loss of coordinate replication of these genomes. Flawed nuclear mitosis was evidenced by cells with abnormally high numbers of kinetoplasts but only 1 or 2 giant nuclei (Figure [2Ci](#) and [2Cii](#)). Conversely, defective kinetoplast segregation, with unchecked nuclear mitosis,

produced cells with multiple nuclei and a single large kinetoplast, demonstrated numerically by the increase in 2N1K cells (Figure [2B](#), [2Ciii](#), and [2Civ](#)). Grouping cells on the basis of the ratio of nuclei to kinetoplasts established kinetoplast segregation as more defective than nuclear mitosis: 29% had more nuclei than kinetoplasts (Figure [2D](#)). Of cells that retained a normal census of nuclei and kinetoplasts, many still had evident dysregulation, including 2N2K cells whose kinetoplasts had begun to rereplicate prior to cytokinesis (Figure [2Cv](#)). Phase contrast confirmed the cytokinesis inhibition suggested by 6C and 8C flow cytometry peaks. At 24 hours, cells with multiple partially ingressed cleavage furrows indicated repeated failed attempts at cell division (Figure [2Ci](#) and [2Ciii](#)), and some cells were arrested at abscission (Figure [2Cvi](#)).

Interestingly, abnormalities from 100 nM 17-AAG were substantially less varied. Although morphologically abnormal ([Supplementary Figure 1E](#)) and with an increased 2N population (including aberrant 2N1K; [Supplementary Figure 1F](#)), few trypanosomes had incomplete cleavage furrows or >2 nuclei or kinetoplasts. In conjunction with flow cytometry results, this suggests strong mitosis inhibition at 24 hours: although 52% of cells had 4C nuclear DNA content, only 28% were 2N, and, conversely, just 8% had 2C DNA content, but 66% were 1N.

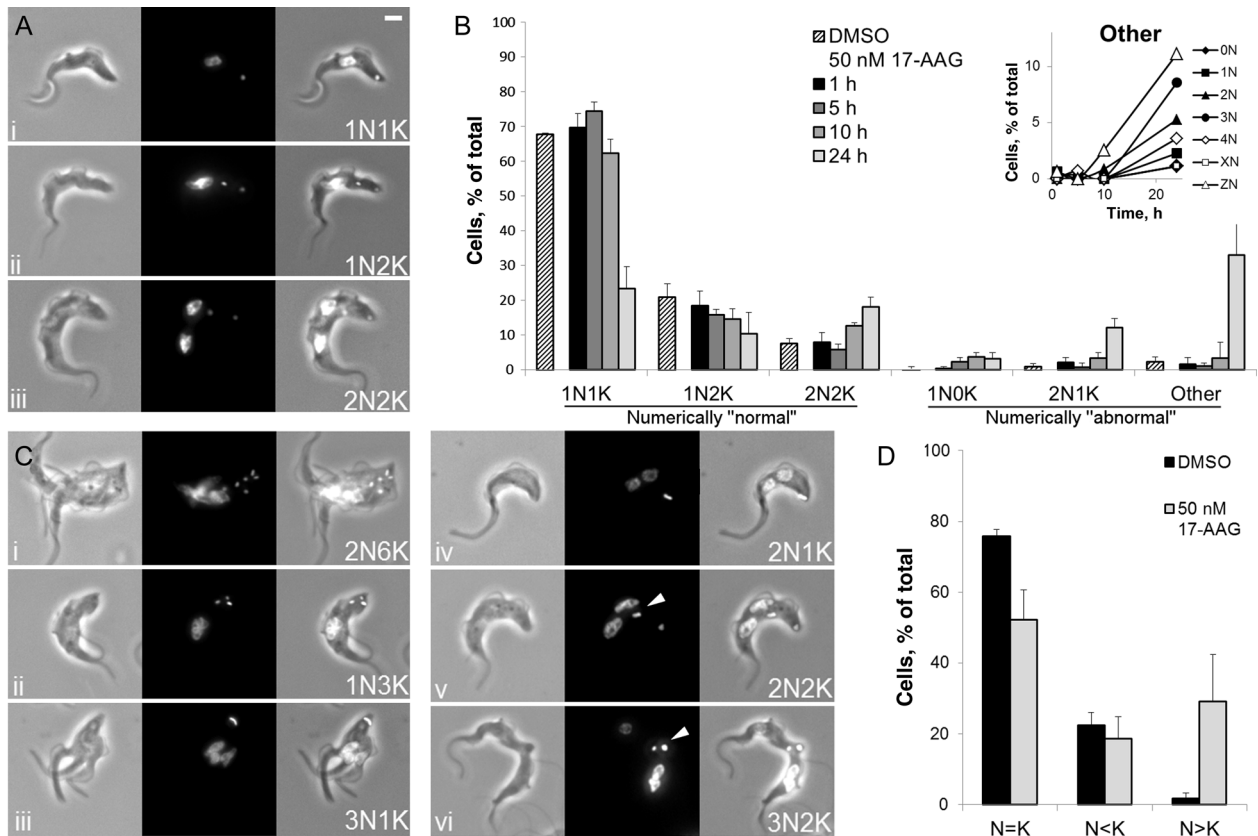


Figure 2. Analyses of trypanosome nuclear and kinetoplast content by DAPI staining and fluorescence microscopy. *A*, Examples, as indicated, of normal 1 nucleus and kinetoplast (1N1K) cells, 1 nucleus and 2 kinetoplast (1N2K) cells, and 2 nuclei and kinetoplast (2N2K) cells in control cultures. Bar, 1 μ m. *B*, Trypanosomes were treated with 50 nM 17-AAG or solvent for the indicated times and then scored for nuclear and kinetoplast content on the basis of DAPI staining. Values are the means \pm SD of counts made in a blinded fashion by 3 observers. The insert shows nuclear content of other cells across time. DMSO, dimethyl sulfoxide; X, ≥ 5 ; Z, not identifiable. *C*, Examples of aberrant cells after 24 hours of treatment with 50 nM 17-AAG. White arrowhead, re-replicating kinetoplast. *D*, Analysis of data from panel *B* to determine the percentage of cells with a number of nuclei equal to, less than, or greater than the number of kinetoplasts.

To test whether structurally different Hsp90 inhibitors caused cell cycle disruption, trypanosomes were treated with 350 nM radicicol (EC₉₉). Patterns comparable to those described above were seen by microscopy and flow cytometry (Supplementary Figure 1G and 1H), indicating the effects are likely attributable to Hsp83 inhibition.

The multiple abnormalities caused by Hsp90 inhibitors suggest that Hsp83 deficiency affects several cell cycle proteins. At submaximal inhibition, the lack of effective checkpoints results in abnormal nuclear and kinetoplast content and abortive cytokinesis. With more stringent inhibition of Hsp83, the regulated ability of cells to initiate DNA segregation and cytokinesis is more severely impaired, which limits the variety of abnormalities. Overall, and in contrast to previous reports involving the insect forms of other kinetoplastids [12–14], these results indicate time- and concentration-dependent disruption of both G₁ and G₂ phases (Figure 1).

Additional Effects of 17-AAG

Heat shock chaperones were initially recognized as proteins whose levels increased after heat stress. Hsp90, among other chaperones, helps maintain protein quality control. We hypothesized that if 17-AAG inhibits Hsp83, then 17-AAG might sensitize trypanosomes to heat shock (Figure 3). In control cells, a heat pulse for one hour caused an arrest in trypanosome cell growth for 10 hours. In a dose-dependent fashion, 17-AAG sensitized trypanosomes to heat shock. Cells shocked in 30 nM 17-AAG (which is ordinarily an EC₃₀) continuously declined in number and did not recover. Other antitrypanosomals with different mechanisms of action, pentamidine and melarsoprol, sensitized trypanosomes to heat shock, but neither was as potent as 17-AAG. Eflornithine had no effect (Supplementary Figure 2).

Somewhat surprisingly, in 2 assays we found that trypanosomes differed from mammalian cells in response to Hsp90

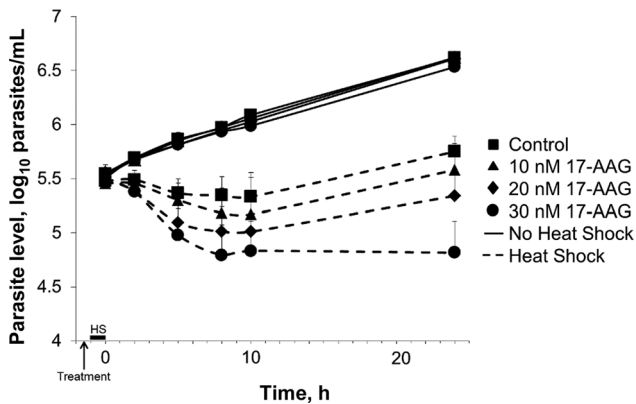


Figure 3. *Trypanosoma brucei* treated with 17-AAG are more sensitive to heat shock. Starting at -1.5 hours, cells at 37°C were treated with 17-AAG or solvent as indicated. The temperature for control cells remained at 37°C for the duration of the experiment. At -1 hour, tubes containing cells to be heat shocked (HS) were transferred to a 41°C water bath and then returned to a 37°C environment at 0 hours for the remainder of the experiment. Motile cells were counted by hemocytometer to determine parasite density. Values are the mean \pm SD of 3 determinations.

inhibitors: we saw no decrease in argonaute protein levels (a mammalian Hsp90 client [33]) and no synergy with other drugs, including etoposide, melarsoprol, pentamidine, or novobiocin (Supplementary Figure 3).

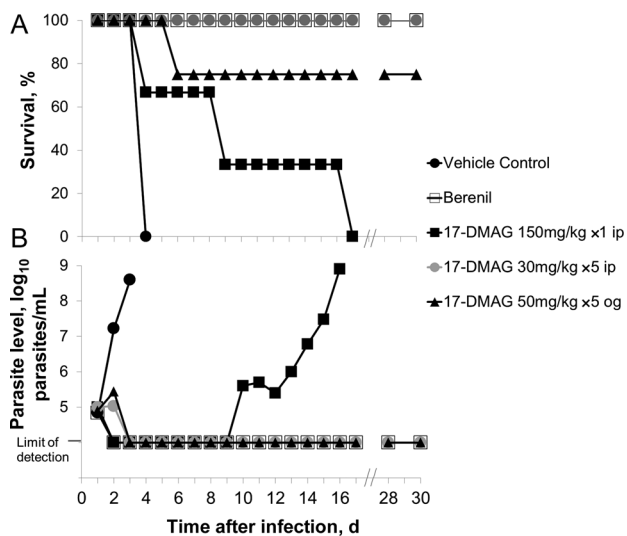


Figure 4. 17-DMAG has antitrypanosomal activity in vivo. Mice were infected with *Trypanosoma brucei* on day 0. Starting on day 1, they were treated once daily with vehicle or drug as indicated and then monitored for up to 30 days for survival (A) and parasitemia (average value for group; B) by visual analysis and hemocytometer counts of trypanosomes in tail snip blood samples. ip, intraperitoneally; og, by oral gavage; $\times 1$, once; $\times 5$, for 5 days.

Activity of 17-DMAG in *T. brucei*-Infected Mice

The promising in vitro cytotoxicity of Hsp90 inhibitors supported evaluation in a mouse model of *T. brucei* infection. 17-DMAG was chosen because of its superior water solubility, potency, and selectivity (Table 2). In this acute model, parasites rapidly proliferated in vehicle controls and caused death within 4 days (Figure 4). The veterinary antitrypanosomal diminazen (Berenil) cured all mice. Three dosing strategies with 17-DMAG provided initial clearance of parasitemia and prolonged survival relative to controls. A single high parenteral dose of 150 mg/kg led to dose-limiting toxicity and day 10 recurrence of parasitemia in the surviving mouse. When this same total dose was divided over 5 days, parasitemia dropped below the lower limit of detection by day 3, and all mice were cured (ie, lacked detectable parasitemia) for 30 days (Figure 4). Of considerable importance, oral 17-DMAG (50 mg/kg daily for 5 days) caused prompt reduction in parasitemia and cured all but 1 mouse, which died on day 6 from gavage-induced trauma and/or drug toxicity. The remaining mice in this group appeared healthy and remained parasite free for 30 days (Figure 4). Weight change as an index of health was consistent with these outcomes. On day 0, the average weight was 21.6 g. Between days 0 and 7, average weight changes were $+2.2$ g (Berenil group), -0.75 g (17-DMAG, 150 mg/kg intraperitoneally once), $+3.5$ g (17-DMAG, 30 mg/kg intraperitoneally for 5 days), and $+3.2$ g (17-DMAG, 50 mg/kg by oral gavage for 5 days).

DISCUSSION

We evaluated Hsp90 inhibitors against bloodstream-form *T. brucei* in vitro and in vivo. Geldanamycin has potent activity in vitro, and orally dosed 17-DMAG cures mice of infection. Is this promising antitrypanosomal activity due to Hsp83 inhibition? Multiple lines of evidence from our laboratory and reported by others suggest that it is. Genetic studies have shown that *T. cruzi* Hsp83 complements an Hsp90 knockout yeast strain [34]. In *L. donovani*, geldanamycin selects Hsp83 from a cosmid library screen, and overexpression of Hsp83 decreases sensitivity to geldanamycin [12]. Biochemical evidence includes geldanamycin-mediated retrieval of Hsp83 from *T. evansi* lysates [16]. With *T. brucei*, we find that the structurally dissimilar Hsp90 inhibitors 17-AAG and radicol cause the same cell cycle dysregulation; that despite important differences, major structural requirements on the ansamycin scaffold are similar for antitrypanosomal and anti-tumor activities; and that 17-AAG sensitizes trypanosomes to heat shock. The antitrypanosomal effects we have shown validate Hsp83 as a drug target in bloodstream-form African trypanosomes.

Less clear are the downstream consequences of Hsp83 inhibition: why does Hsp83 deficiency kill trypanosomes? In higher eukaryotes, the toxicity of Hsp90 inhibitors is attributed to

subsequent functional loss of client proteins, which include key cell cycle regulators. We find vivid evidence of cell cycle dysregulation in trypanosomes treated with Hsp90 inhibitors. Many gene products essential for orderly progression through the trypanosome cell cycle have been identified via RNA interference silencing, including kinases (eg, cyclin-related, Aurora, Polo-like [35–37]) and kinase regulators (eg, cyclins, kinase activator MOB1, and kinase receptor TRACK [38–40]), several of whose mammalian homologs are recognized Hsp90 clients [41–44]. Individual knockdown of these proteins in kinetoplastids generates a cell cycle defect, such as abnormal numbers of kinetoplasts or nuclei and arrested or misplaced cleavage furrows. Unlike these discrete phenotypes, however, with Hsp90 inhibitors we see multiple abnormalities in the same cell and pleomorphic abnormalities in the population (Figure 2C). These complex and profound disruptions of nuclear and kinetoplast segregation and cytokinesis support the notion that Hsp83, like Hsp90 in higher eukaryotes, is an important node in the midst of numerous regulatory pathways.

In the development of any antiparasitic drug, a critical consideration is therapeutic index. Our findings that trypanosomes and L1210 tumor cells differ in susceptibility to Hsp90 inhibitors and, more importantly, that 17-DMAG cures mice of *T. brucei* infection provide convincing evidence that Hsp90 inhibitors can be selectively toxic for trypanosomes. Given the 61% protein sequence identity between Hsp90 and Hsp83, it is interesting to speculate about the basis for this discrimination. Precedent for selective toxicity to Hsp90 inhibitors exists in the greater susceptibility (up to 200-fold) of tumor cells as compared to nontransformed cells [8, 45]. Cancer cells are thought to be unusually dependent on Hsp90 to chaperone upregulated oncogene clients and mutant proteins and to counter the toxic metabolic environment commonly present in tumors [5–8]. Many factors could heighten susceptibility of trypanosomes to Hsp90 inhibitors, including the previously suggested differences in inhibitor binding affinity at the ATPase site, or less stringent checkpoints lowering the threshold for cell cycle disruption. However, the unique cellular pathways in these ancient eukaryotes suggest other downstream processes, not present in host cells, that may be unusually dependent on Hsp83. These include the heat shock-sensitive requisite *trans*-splicing of a 5'-leader sequence onto all messenger RNAs [46] (the disruption of which would globally cripple protein synthesis) or the production of essential variable surface glycoprotein for the cell surface coat (which requires chaperone activity) [47, 48].

Extensive studies of Hsp90 inhibitors in humans provide a strong starting point for their possible use in African trypanosomiasis. In phase 1 trials of 17-DMAG, maximum tolerated doses generated maximum blood concentrations of 600–2700 nM [49, 50], well in excess of the 3 nM EC₅₀ against trypanosomes in vitro (Table 2). Distinctly different susceptibilities and doubling times of trypanosomes and mammalian cells

suggest that doses and prolonged regimens suitable for cancer therapy may be inappropriate for trypanosomiasis; indeed, our mouse study indicates that limited regimens may suffice. Furthermore, there are 16 other Hsp90 inhibitors currently in clinical trials, several of which have better safety profiles than 17-DMAG and 7 of which are administered orally [7].

We have demonstrated that Hsp90 inhibitors in vitro cause potent growth inhibition of *T. brucei* and vivid morphological abnormalities and that oral dosing cures trypanosomiasis in mice. In the laboratory, these agents provide a valuable tool for studying the role of Hsp83 in kinetoplastids. More importantly, good clinical promise is afforded by the numerous Hsp90 inhibitors now in human trials. Our results support further investigation into the repurposing of Hsp90 inhibitors as antitrypanosomal agents.

Supplementary Data

Supplementary materials are available at *The Journal of Infectious Diseases* online (<http://jid.oxfordjournals.org/>). Supplementary materials consist of data provided by the author that are published to benefit the reader. The posted materials are not copyedited. The contents of all supplementary data are the sole responsibility of the authors. Questions or messages regarding errors should be addressed to the author.

Notes

Acknowledgments. We thank Rahul Bakshi, Elizabeth Nenortas, and Calvin Tiengwe, for technical support; Elizabetta Ullu, for the generous gift of Ago1 antibody; Rahul Bakshi, Paul Englund, Rob Jensen, and Elizabeth Nenortas, for comments on the manuscript; and Caren Freil Meyers, for comments on the SAR section. Instrument support was provided by the Becton Dickinson Immune Function Laboratory of the Flow Cytometry Core, Johns Hopkins Bloomberg School of Public Health. This work would not have been possible without the provision of compounds by the Open Chemical Repository of the Drug Synthesis and Chemistry Branch, Developmental Therapeutics Program, Division of Cancer Treatment and Diagnosis, National Cancer Institute (available at: <http://dtp.cancer.gov>).

Financial support. This work was supported by the National Institutes of Health (grants R01AI028855-16 and R01AI095453 to T. S.) and Fulbright New Zealand (Fulbright, Ministry of Research Science and Technology, Graduate Award to K. M.).

Potential conflicts of interest. All authors: No reported conflicts.

All authors have submitted the ICMJE Form for Disclosure of Potential Conflicts of Interest. Conflicts that the editors consider relevant to the content of the manuscript have been disclosed.

References

1. Brun R, Blum J, Chappuis F, Burri C. Human African trypanosomiasis. *Lancet* **2010**; 375:148–59.
2. Taipale M, Jarosz DF, Lindquist S. Hsp90 at the hub of protein homeostasis: emerging mechanistic insights. *Nat Rev Mol Cell Biol* **2010**; 11:515–28.
3. Kaplan KB, Li R. A prescription for “stress”—the role of Hsp90 in genome stability and cellular adaptation. *Trends Cell Biol* **2012**; 22:576–83.
4. Li J, Soroka J, Buchner J. The Hsp90 chaperone machinery: conformational dynamics and regulation by co-chaperones. *Biochim Biophys Acta* **2012**; 1823:624–35.

5. Trepel J, Mollapour M, Giaccone G, Neckers L. Targeting the dynamic Hsp90 complex in cancer. *Nat Rev Cancer* **2010**; 10:537–49.
6. Whitesell L, Lin NU. Hsp90 as a platform for the assembly of more effective cancer chemotherapy. *Biochim Biophys Acta* **2012**; 1823:756–66.
7. Travers J, Sharp S, Workman P. Hsp90 inhibition: two-pronged exploitation of cancer dependencies. *Drug Discov Today* **2012**; 17:242–52.
8. Kamal A, Thao L, Sensintaffar J, et al. A high-affinity conformation of Hsp90 confers tumour selectivity on Hsp90 inhibitors. *Nature* **2003**; 425:407–10.
9. Matts RL, Brandt GE, Lu Y, et al. A systematic protocol for the characterization of Hsp90 modulators. *Bioorg Med Chem* **2011**; 19:684–92.
10. Lu X, Xiao L, Wang L, Ruden DM. Hsp90 inhibitors and drug resistance in cancer: the potential benefits of combination therapies of Hsp90 inhibitors and other anti-cancer drugs. *Biochem Pharmacol* **2012**; 83:995–1004.
11. Mottram JC, Murphy WJ, Agabian N. A transcriptional analysis of the *Trypanosoma brucei* Hsp83 gene cluster. *Mol Biochem Parasitol* **1989**; 37:115–27.
12. Wiesgigl M, Clos J. Heat shock protein 90 homeostasis controls stage differentiation in *Leishmania donovani*. *Mol Biol Cell* **2001**; 12:3307–16.
13. Graefe SEB, Wiesgigl M, Gaworski I, Macdonald A, Clos J. Inhibition of Hsp90 in *Trypanosoma cruzi* induces a stress response but no stage differentiation. *Eukaryot Cell* **2002**; 1:936–43.
14. Li Q, Zhou Y, Yao C, et al. Apoptosis caused by Hsp90 inhibitor geldanamycin in *Leishmania donovani* during promastigote-to-amastigote transformation stage. *Parasitol Res* **2009**; 105:1539–48.
15. Jones C, Anderson S, Singha UK, Chaudhuri M. Protein phosphatase 5 is required for Hsp90 function during proteotoxic stresses in *Trypanosoma brucei*. *Parasitol Res* **2008**; 102:835–44.
16. Pallavi R, Roy N, Nageshan RK, et al. Heat shock protein 90 as a drug target against protozoan infections: biochemical characterization of Hsp90 from *Plasmodium falciparum* and *Trypanosoma evansi* and evaluation of its inhibitor as a candidate drug. *J Biol Chem* **2010**; 285:37964–75.
17. Adriano MA, Vergnes B, Poncet J, et al. Proof of interaction between *Leishmania* Sir2RFP1 deacetylase and chaperone Hsp83. *Parasitol Res* **2007**; 100:811–8.
18. Parsons M, Worthey EA, Ward PN, Mottram JC. Comparative analysis of the kinomes of three pathogenic trypanosomatids: *Leishmania major*, *Trypanosoma brucei* and *Trypanosoma cruzi*. *BMC Genomics* **2005**; 6:127.
19. Nett IR, Martin DM, Miranda-Saavedra D, et al. The phosphoproteome of bloodstream form *Trypanosoma brucei*, causative agent of African sleeping sickness. *Mol Cell Proteomics* **2009**; 8:1527–38.
20. Woodward R, Gull K. Timing of nuclear and kinetoplast DNA replication and early morphological events in the cell cycle of *Trypanosoma brucei*. *J Cell Sci* **1990**; 95(Pt 1):49–57.
21. Jensen RE, Englund PT. Network news: the replication of kinetoplast DNA. *Annu Rev Microbiol* **2012**; 66:473–91.
22. McKean PG. Coordination of cell cycle and cytokinesis in *Trypanosoma brucei*. *Curr Opin Microbiol* **2003**; 6:600–7.
23. Hammarton TC. Cell cycle regulation in *Trypanosoma brucei*. *Mol Biochem Parasitol* **2007**; 153:1–8.
24. Li Z. Regulation of the cell division cycle in *Trypanosoma brucei*. *Eukaryot Cell* **2012**; 11:1180–90.
25. Bodley AL, McGarry MW, Shapiro TA. Drug cytotoxicity assay for African trypanosomes and *Leishmania* species. *J Infect Dis* **1995**; 172:1157–9.
26. Field MC, Allen CL, Dhir V, et al. New approaches to the microscopic imaging of *Trypanosoma brucei*. *Microsc Microanal* **2004**; 10:621–36.
27. Grenert JP, Sullivan WP, Fadden P, et al. The amino-terminal domain of heat shock protein 90 (Hsp90) that binds geldanamycin is an ATP/ADP switch domain that regulates Hsp90 conformation. *J Biol Chem* **1997**; 272:23843–50.
28. Schulte TW, Akinaga S, Soga S, et al. Antibiotic radicicol binds to the N-terminal domain of Hsp90 and shares important biologic activities with geldanamycin. *Cell Stress Chaperones* **1998**; 3:100–8.
29. Marcu MG, Chadli A, Bouhouche I, Catelli M, Neckers LM. The heat shock protein 90 antagonist novobiocin interacts with a previously unrecognized ATP-binding domain in the carboxyl terminus of the chaperone. *J Biol Chem* **2000**; 275:37181–6.
30. Johnson VA, Singh EK, Nazarova LA, Alexander LD, McAlpine SR. Macrocyclic inhibitors of Hsp90. *Curr Top Med Chem* **2010**; 10:1380–402.
31. Nadeau K, Sullivan MA, Bradley M, Engman DM, Walsh CT. 83-kilodalton heat shock proteins of trypanosomes are potent peptide-stimulated ATPases. *Protein Sci* **1992**; 1:970–9.
32. Borst P, van der Ploeg M, van Hoek JF, Tas J, James J. On the DNA content and ploidy of trypanosomes. *Mol Biochem Parasitol* **1982**; 6:13–23.
33. Pare JM, Tahbaz N, Lopez-Orozco J, LaPointe P, Lasko P, Hobman TC. Hsp90 regulates the function of argonaute 2 and its recruitment to stress granules and P-bodies. *Mol Biol Cell* **2009**; 20:3273–84.
34. Palmer G, Louvion JF, Tibbetts RS, Engman DM, Picard D. *Trypanosoma cruzi* heat shock protein 90 can functionally complement yeast. *Mol Biochem Parasitol* **1995**; 70:199–202.
35. Tu X, Wang CC. The involvement of two cdc2-related kinases (CRKs) in *Trypanosoma brucei* cell cycle regulation and the distinctive stage-specific phenotypes caused by CRK3 depletion. *J Biol Chem* **2004**; 279:20519–28.
36. Tu X, Kumar P, Li Z, Wang CC. An aurora kinase homologue is involved in regulating both mitosis and cytokinesis in *Trypanosoma brucei*. *J Biol Chem* **2006**; 281:9677–87.
37. Hammarton TC, Kramer S, Tetley L, Boshart M, Mottram JC. *Trypanosoma brucei* Polo-like kinase is essential for basal body duplication, kDNA segregation and cytokinesis. *Mol Microbiol* **2007**; 65:1229–48.
38. Hammarton TC, Clark J, Douglas F, Boshart M, Mottram JC. Stage-specific differences in cell cycle control in *Trypanosoma brucei* revealed by RNA interference of a mitotic cyclin. *J Biol Chem* **2003**; 278:22877–86.
39. Hammarton TC, Lillico SG, Welburn SC, Mottram JC. *Trypanosoma brucei* MOB1 is required for accurate and efficient cytokinesis but not for exit from mitosis. *Mol Microbiol* **2005**; 56:104–16.
40. Rothberg KG, Burdette DL, Pfannstiel J, Jetton N, Singh R, Ruben L. The RACK1 homologue from *Trypanosoma brucei* is required for the onset and progression of cytokinesis. *J Biol Chem* **2006**; 281:9781–90.
41. Lange BMH, Rebollo E, Herold A, Gonzalez C. Cdc37 is essential for chromosome segregation and cytokinesis in higher eukaryotes. *Embo J* **2002**; 21:5364–74.
42. Caldas-Lopes E, Cerchietti L, Ahn JH, et al. Hsp90 inhibitor PU-H71, a multimodal inhibitor of malignancy, induces complete responses in triple-negative breast cancer models. *Proc Natl Acad Sci U S A* **2009**; 106:8368–73.
43. Simizu S, Osada H. Mutations in the Plk gene lead to instability of Plk protein in human tumour cell lines. *Nat Cell Biol* **2000**; 2:852–4.
44. Basto R, Gergely F, Draviam VM, Ohkura H, Liley K, Raff JW. Hsp90 is required to localise cyclin B and Msps/ch-TOG to the mitotic spindle in *Drosophila* and humans. *J Cell Sci* **2007**; 120:1278–87.
45. Amolins MW, Blagg BS. Natural product inhibitors of Hsp90: potential leads for drug discovery. *Mini Rev Med Chem* **2009**; 9:140–52.
46. Muhich ML, Boothroyd JC. Polycistronic transcripts in trypanosomes and their accumulation during heat-shock - evidence for a precursor role in messenger-RNA synthesis. *Mol Cell Biol* **1988**; 8:3837–46.
47. Bangs JD, Brouch EM, Ransom DM, Roggy JL. A soluble secretory reporter system in *Trypanosoma brucei*. Studies on endoplasmic reticulum targeting. *J Biol Chem* **1996**; 271:18387–93.
48. Descoteaux A, Avila HA, Zhang K, Turco SJ, Beverley SM. *Leishmania* LPG3 encodes a GRP94 homolog required for phosphoglycan synthesis implicated in parasite virulence but not viability. *Embo J* **2002**; 21:4458–69.

49. Ramanathan RK, Egorin MJ, Erlichman C, et al. Phase I pharmacokinetic and pharmacodynamic study of 17-dimethylaminoethylamino-17-demethoxygeldanamycin, an inhibitor of heat-shock protein 90, in patients with advanced solid tumors. *J Clin Oncol* **2010**; 28:1520–6.
50. Pacey S, Wilson RH, Walton M, et al. A phase I study of the heat shock protein 90 inhibitor alvespimycin (17-DMAG) given intravenously to patients with advanced solid tumors. *Clin Cancer Res* **2011**; 17:1561–70.